A fluid-structure interaction model for heart valves with a single degree of freedom

A Fluid–Structure Interaction Model for Heart Valves with a Single Degree of Freedom

J.B.A.M. Horsten, A.A. van Steenhoven and D.H. van Campen

Department of Mechanical Engineering
Eindhoven University of Technology
P.O.Box 513, 5600 MB Eindhoven, The Netherlands

Summary

As a preparatory study for the analysis of the opening and closing behavior of aortic valve prostheses in a viscous fluid flow, a rigid two–dimensional valve, which can rotate around its point of attachment is analyzed. The valve motion and the fluid velocity field are computed. The equations of motion for fluid and structure are iteratively coupled. For the fluid the full unsteady 2D incompressible Navier–Stokes equations are solved. The valve is assumed to be rigid and its inertia is neglected. The equilibrium position of the valve at a point of time is found iteratively, using the Van Wijngaarden–Dekker–Brent method for the root–finding of a nonlinear equation. The numerical method is validated by means of measurement of the interaction forces and the valve displacement in an experimental model. A comparison of numerical and experimental results show that a proper method is developed.

Introduction

Frequently, natural human aortic valves do not function properly and need to be replaced by valve prostheses. An important feature of the natural valve is its partial closure during flow deceleration, such that the reverse flow back into the heart is minimized [1]. This condition is not satisfied by the commonly used disc–type valve prostheses, which consist of one or two rigid plates, mounted in frame [2]. For the design of an improved disc–type aortic valve prosthesis the valvular opening and closing need to be investigated.

Several models for this problem have been developed. Most of them are analytical ones, based on a quasi–one–dimensional approach [1,3,4]. These models give a fair global description of the valve motion, notwithstanding a strong simplification of the fluid flow phenomena, but they cannot give an analysis of the effect of small variations of the valve geometry. A a much more detailed numerical model, specially developed for heart valves, is given by Peskin [5]. It incorporates the full Navier–Stokes equations and flexible boundaries. A major drawback of this model is its limited stability, due to an explicit estimation of the fluid–valve interaction terms. Furthermore, the Reynolds number and spatial accuracy are limited and rigid boundaries can only be incorporated in an indirect way. Somewhat more general fluid–structure interaction models, of which overviews are given in [6] and [7], are not suitable for our purpose, since they generally simplify the fluid flow too much and the inertia of the structure is essential for those models. In our case the situation is opposite: the inertia of natural heart valves is negligible compared to that of surrounding blood.

The object of this study is the development of a numerical fluid–structure interaction model, allowing for a full description of laminar flow patterns in complex

domains and for general rigid body structures. In the present model the structure is restricted to have only one degree of freedom and a negligible inertia. However, inertial effects can easily be incorporated. The model valve is shown in figure 1. It is rigid and can rotate around its point of attachment. Behind the disc a cylindrical cavity is present, which is a modeled version of the physiological sinus of Valsalva. The valve is attached to the rigid channel by a membranous hinge. This hinge causes a bending moment in the direction of the closed position. The valve is partly hollow and the average density is 0.95 times that of water, the fluid which is used, so a buoyancy force is acting to the fully opened position. The magnitude of these forces is chosen such that they are in equilibrium for $\varphi \approx 13^{o}$. The channel width is six times its height in order to minimize three dimensional effects. The fluid flow is assumed to be Newtonian, incompressible, two—dimensional and laminar. Although physiological Reynolds numbers are larger (Re=4000), for computational reasons the maximum Reynolds number was chosen to be 800. The interaction will be taken fully into account. The equations of motion for fluid and structure are iteratively coupled. The subsystems are evaluated separately and an iteration procedure is applied until equilibrium is achieved.

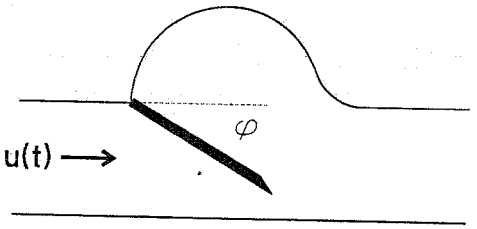

fig.1 Two—dimensional model of the aortic valve

Fluid model

Flow of an incompressible, Newtonian and isothermal fluid must satisfy the Navier—Stokes and continuity equations. In dimensionless form these equations read:

$$St\,\dot{\vec{u}} + \vec{u}\cdot\nabla\vec{u} - \frac{1}{Re}\nabla^2\vec{u} + \nabla p - \vec{f} = \vec{0} \qquad (1a)$$

$$\nabla\cdot\vec{u} = 0 \qquad (1b)$$

with $\vec{u}$ the velocity vector, p the pressure, $\vec{f}$ the body force per unit mass, ∇ the gradient vector operator and the superscript dot $\cdot$ denotes the local time derivative. St denotes the Strouhal number defined as $St = h/u\tau$ with τ a characteristic time scale, h the channel height and u the mean axial velocity. Re is the Reynolds number, defined as $Re = uh/\nu$ with ν the kinematic viscosity.

To obtain an approximation of the velocity and the pressure field within a domain Ω, a standard Galerkin finite element method is applied. Here, only a brief synopsis of the method is given. More details can be found elsewhere [8,10]. A 7—noded triangular Crouzeix—Raviart element, as showed in figure 2, is used. The basis functions of the velocity are extended quadratic functions. Velocity unknowns are defined in all the nodal points. Pressure unknowns are only defined in the center of the element, which are the pressure itself and its three spatial derivatives. The basis functions of the pressure are linear and discontinuous over the element boundaries. The velocity unknowns and the pressure derivatives within the centroid of the element are

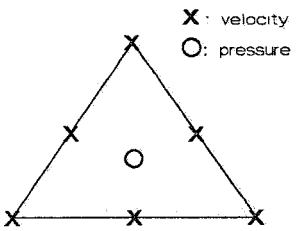

fig.2 Modified $p_2^+ - p_1$ Crouzeix—Raviart element for the spatial discretisation of the Navier—Stokes equations

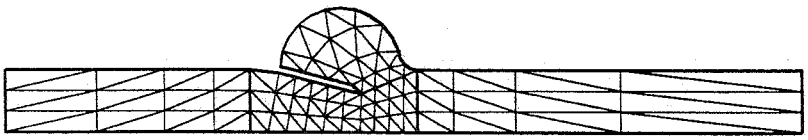

fig.3 Finite element mesh for the fluid flow analysis in the aorta model

eliminated by consideration of the Navier—Stokes and continuity equations elementwise. This leads to a total amount of unknowns of 13. It can be shown that the element satisfies the Babuska—Brezzi condition. The accuracy of the velocity is of order Δx^3 and that of the pressure of order Δx^2, with Δx a characteristic element size. An example of a typical element mesh is given in figure 3.

The spatial discretization leads to a set of matrix equations:

$$\underline{M}\,\dot{\underline{u}} + [\underline{S} + \underline{N}(\underline{u})]\underline{u} + \underline{L}^T\underline{p} = \underline{f} + \underline{b} \qquad (2a)$$

$$\underline{L}\,\underline{u} = \underline{0} \qquad (2b)$$

where $\underline{M}\,\dot{\underline{u}}$ represents the local acceleration term, $\underline{L}^T\underline{p}$ the pressure gradient term, Su the viscous term, $N(\underline{u})\,\underline{u}$ the convective acceleration term and $\underline{L}\,\underline{u}$ the velocity divergence term. $\underline{f}$ and $\underline{b}$ represent the volume and boundary forces respectively. $\underline{u}$ contains the velocity and $\underline{p}$ the pressure unknowns in the nodal points. In the set of equations (2) the pressure unknowns do not occur in the continuity equation This leads to zero diagonal elements. In order to avoid partial pivoting and to reduce the number of unknowns, a penalty function method is applied. The discretized continuity equation is replaced by:

$$\underline{L}\,\underline{u} = \varepsilon\,\underline{M}_p\,\underline{p} \qquad (3)$$

with $\underline{M}_p$ the pressure matrix and ε a very small parameter. If the right hand side of eq. (3) is small enough, then the incompressibility of the fluid will be sufficiently approximated. For the problems solved in this study the value of ε was chosen to be $\varepsilon = 10^{-6}$, which leads to values of $\varepsilon\,\underline{M}_p\,\underline{p}$ of $O(10^{-6})$ in the dimensionless formulation.

The local time derivative in (2) is approximated by the Euler—implicit scheme:

$$\dot{\underline{u}}^{n+1} = \frac{\underline{u}^{n+1} - \underline{u}^n}{\Delta t} \qquad (4)$$

in which $\underline{u}^n$ is an abbreviation for $\underline{u}(n\Delta t)$ with Δt the time step. This scheme is unconditionally stable and first order accurate in time. Although a Crank—Nicolson scheme would be more accurate than the Euler—implicit scheme, the latter will be used in this study. The motivation is found in the observation that, for reasons which are not completely clear yet, the computed pressure shows small oscillations round the correct values if a Crank—Nicolson scheme is used [10]. The restriction to a first order scheme is not inherent to the fluid—structure interaction algorithm itself (there are no objections for a higher order scheme), but it is a result of a limitation of the fluid solver.

The non—linear convective term $\underline{\underline{N}}(\underline{u})\underline{u}$ in (2a) is linearized by a Newton—Raphson iteration scheme:

$$\underline{\underline{N}}(\underline{u}^{i+1})\,\underline{u}^{i+1} = \underline{\underline{J}}(\underline{u}^i)\,\underline{u}^{i+1} - \underline{\underline{N}}(\underline{u}^i)\,\underline{u}^i \tag{5}$$

with i the index of the iteration step and $\underline{\underline{J}}(\underline{u})$ the Jacobian matrix of $\underline{\underline{N}}(\underline{u})\underline{u}$. Substituting equations (3), (4) and (5) into (2) leads to the final set of equations:

$$\left[\underline{\underline{M}}/\Delta t + \underline{\underline{S}} + \underline{\underline{J}}(\underline{u}^{n+1,i}) + \varepsilon \underline{\underline{L}}^T \underline{\underline{M}}_p^{-1} \underline{\underline{L}}\right] \underline{u}^{n+1,i+1} = \underline{\underline{M}}/\Delta t\, \underline{u}^n + \underline{\underline{N}}(\underline{u}^{n+1,i})\,\underline{u}^{n+1,i} + \underline{f}^{n+1} + \underline{b}^{n+1}\,. \tag{6}$$

At every time step a full Newton—Raphson iteration is carried out until

$$\max_j \|u_j^{i+1} - u_j^i\| < \delta$$

with $\delta = 10^{-4}$. At every iteration step the system (6) is built and a LU—decomposition is used to solve it. Experiments with simplified Newton schemes, when the Jacobian matrix is not updated every iteration step, did not result in a decreasing computing time.

After convergence the pressure at t_{n+1} is found with eq. (3) and the normal and tangential stresses are interpolated to the element vertices. The total fluid moment acting on the valve is obtained by integrating the local stress over the valve. A trapezoidal rule is used with the element vertices as integration points. The elements on the valve are chosen of equal size, since this results in the optimal accuracy for the integration of the stresses.

As initial condition, the steady state solution for a fully opened valve is taken. As contact condition on the valve, the normal fluid velocity is set equal to the local valve velocity, determined from the actual valve position and that at the previous point of time. The tangential fluid velocity satisfies a no—slip condition. At the entrance, a fully developed parabolic axial velocity profile is prescribed and the radial flow is set to zero. The entrance channel long enough to garantuee a full development of the unsteady velocity profile. At the outflow a stress free flow condition is prescribed.

Structure model

Since its inertia is assumed to be negligible, the structure is in equilibrium if it satisfies the condition:

$$\Sigma m = m_f + m_g + m_b = 0 \tag{7}$$

where m_f is the fluid moment and m_g the moment due to the buoyancy force

$$m_g = g \cos(\varphi) \int_0^l \Delta\rho(s)\, b(s)\, s\, ds \qquad (8)$$

with l and b the length and thickness of the valve respectively, s the coordinate along the valve, g the acceleration of gravity and $\Delta\rho$ the density difference between valve and fluid. m_b is the bending moment in the point of attachment

$$m_b = -k(\varphi_o - \varphi) \qquad (9)$$

with k a bending stiffness parameter and φ_o the angle of fixation of the membranous hinge. At a given point of time, with given inflow conditions and known fluid history, the resulting moment is a function of the unknown valve position φ only. The equilibrium position is the root of the nonlinear equation (7). The derivatives of (7) with respect to φ cannot be computed in a simple way. Therefore, an iterative method is necessary, which does not need the evaluations of the derivatives. Here, the Van Wijngaarden—Dekker—Brent method is used [12,13]. This method assumes that a root is known to be bracketed in a given interval. Then it locates the root, within a given accuracy, by a combination of successive inverse quadratic interpolation and bisection. The method converges never much slower than bisection does and converges superlinear near roots of well—behaved functions.

The bracketing of the root is performed by a restricted extrapolation. As first estimate the solution of the previous time step is taken. The sign of the moment is tested and the second estimate is a trial step in the direction in which the valve is being pushed. Then a linear extrapolation is performed and the next estimate is taken somewhat further than the zero crossing of the extrapolating line. Not the zero crossing is taken, because in this stage only the bracketing is important. Both the extrapolating step and the extrapolated position are restricted to predefined limits. Successive linear extrapolation is performed until the root is bracketed. Always, the two most recent estimates are used. Since the moment appears to be a monotonic function of φ and only extrapolation takes place, they are the closest to the root.

In every timestep, a bracketing and iteration procedure is performed. For each valve position estimate, the mesh is updated and the fluid flow field is computed. The resulting algorithm is fully implicit and hence unconditional numerical stability is achieved. The model is implemented in the SEPRAN software package [9]. The computations are carried out on an Apollo—DN3000 minicomputer and on an Alliant FX/4 mini—supercomputer with two parallel vector processors. The number of position estimates per timestep varies from five to eight. Per position estimate between two and eight Newton iteration steps are necessary. For the typical number of velocity unknowns of 721, this results in about 30 minutes computing time per time step on the Apollo system and about 2 minutes on the Alliant system,

Experiments

The numerical method is validated by means of measurement of the fluid moment acting on the valve and the displacement of the valve as a function of Reynolds number and time. The experimental setup is shown in figure 4. The fluid moment is measured with a force transducer (LVDT) mounted on the upper side of the valve. The valve motion is recorded with a standard video system. The accuracy of the computation of the fluid velocity field has been extensively tested earlier [10,11].

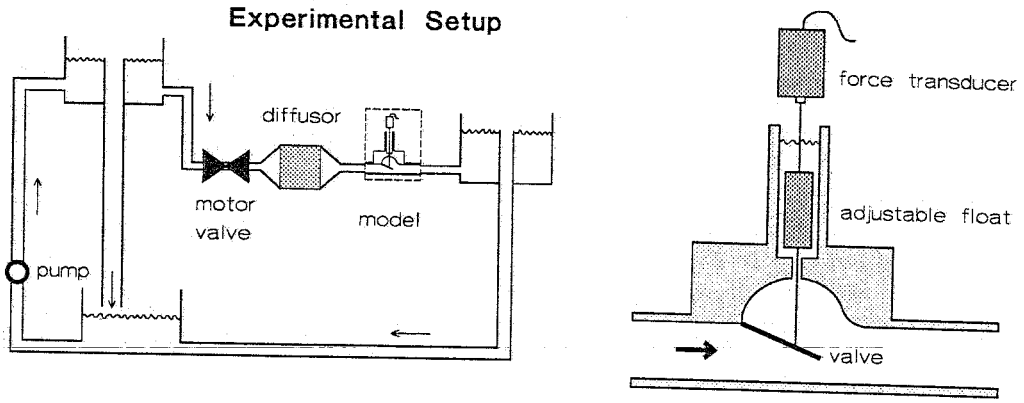

fig.4 Experimental setup: (a) flow channel (b) detail of model

Results

With this method the fluid flow and the valve rotation under steady and pulsating inflow conditions are simulated. A typical result for the steady fluid flow is presented in figure 5. The flow separates at the valve tip and reattaches again at a distance of about the sinus diameter. Behind the valve, a weak vortex is present. The pressure in the sinus is almost constant and equal to that at the valve tip. Figure 6 shows the flow in case of a valve moving towards its closed position under steady inflow conditions. The contents of the sinus rotates together with the valve. This observation supports the negligence of the valve inertia, since it is much smaller than that of the moving fluid.

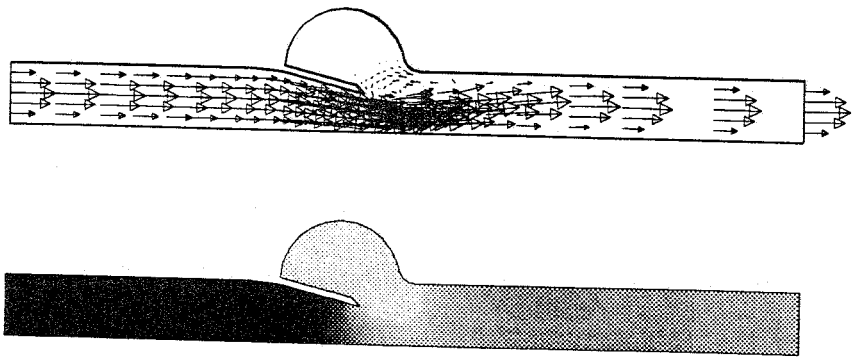

fig.5 Velocity field and pressure distribution for a fixed valve in a steady flow (Re=200)

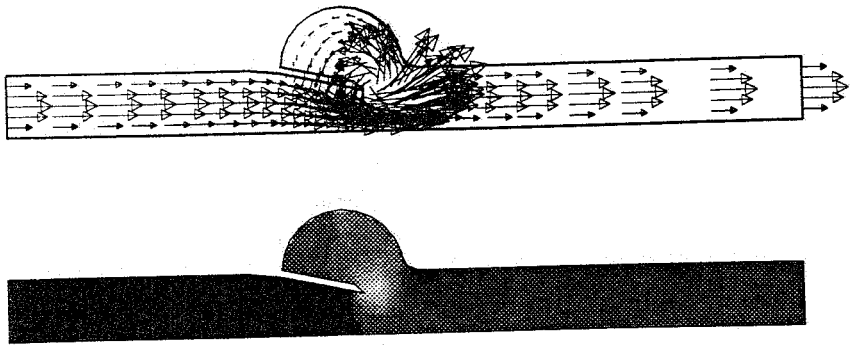

fig.6 Velocity field and pressure distribution for moving valve in a steady flow (Re= 200,St= 1.0)

The computation of the fluid moment is verified in the case that the valve is held in a fixed position, the force transducer being mounted on it. A comparison of numerical and experimental data is given in figure 7. The agreement is close: differences are well within the experimental accuracy limits. Next, the equilibrium position of a freely moving valve in a steady flow is studied as function of the Reynolds number. A preliminary result is given in figure 8. The agreement is not as close as might be expected from figure 7. This deviation is caused by the bending moment in the point of attachment. As stated in eq. (9), it is assumed that the bending parameter is constant. This appears not to hold exactly. More detailed experiments are planned to determine k as a function of the valve position. Also the valve motion due to gravity and bending force in case of a steady inflow is studied. The valve is fixed in its fully opened position till t=0 and then released. The valve rotation is studied at various values of Reynolds number. An example is given in figure 9. Both experimental and numerical results show a second order subcritically damped behavior. The agreement between experimental and numerical results of both the valve motion and the steady equilibrium position is fair. The steady equilibrium positions are the same is in figure 8. The agreement for the valve motion improves if the timestep of the integration is decreased. This indicates that a part of the deviations between theory and experiment is caused by numerical damping, resulting from the first order implicit time integration scheme. Furthermore, the earlier mentioned deviations in the bending stiffness parameter of the membranous hinge may explain some of the observed differences.

Next, valve motion due to volume flow variations at the inlet is studied numerically. A result is given in figure 10. It appears that during flow deceleration the model valve moves already towards its closed position, just like the natural aortic valve does. This early state closure is not observed for commercially available disc—valve prostheses [2]. Experimental verification of this pulsating flow situation is planned.

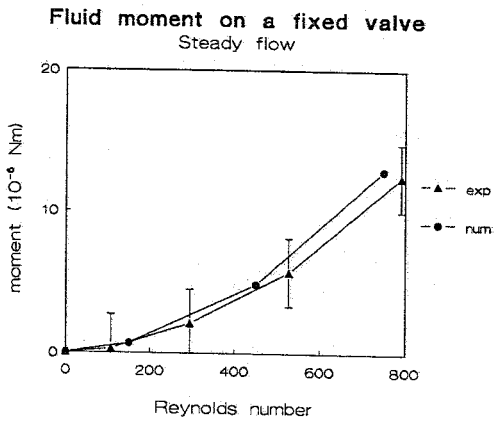

fig.7

Comparison of experimental and numerical moments on a fixed valve due to a steady fluid flow as a function of the Reynolds number ($\varphi = 10^{o}$)

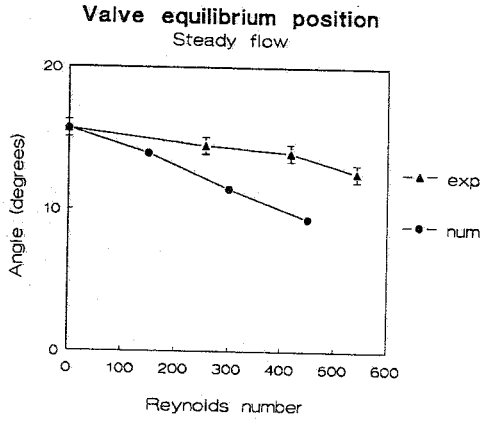

fig.8

Comparison of experimental and numerical valve equilibrium position in a steady flow as a function of the Reynolds number

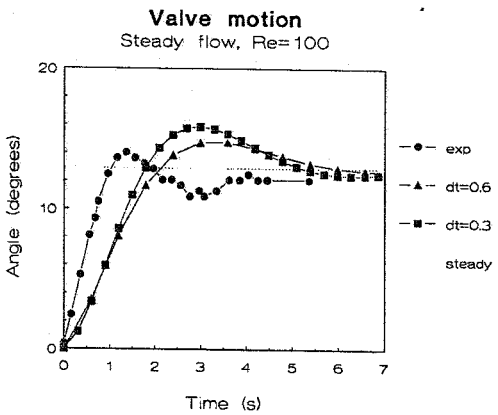

fig.9

Comparison of experimental and numerical valve motion due to gravity and bending force in a steady flow (Re=100). At t=0 the valve is released from the fully opened position.

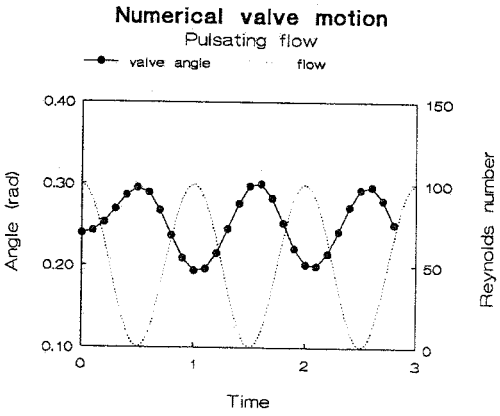

fig.10

Results of a numerical simulation of the valve motion due to a harmonic volume flow variation at the inlet (Re=0—100, St=1))

Concluding discussion

In conclusion, it is stated that a proper method is developed for the numerical analysis of the fluid flow around and the motion of a rigid body with one degree of freedom. The agreement between numerical and experimental results is fair. The method is very flexible, since the structure equilibrium condition (3) can easily be modified and any fluid solver can be used, as long as the velocity and pressure fields are evaluated with sufficient accuracy. For numerical reasons, the study has been performed for a maximum Reynolds number of 800. A qualitative comparison of the obtained results with experimental ones at a higher Reynolds number [1] shows the same characteristics of the flow field. Hence, the present method is valuable for the analysis of the actual situation. On the other hand, some increase of the Reynolds number is possible with the fluid solver used.

In this study inertial effects of the structure are neglected, but they can easily be incorporated by extending of the equilibrium condition (7) to the familiar

$$\Sigma m + I\,\ddot{\varphi} = 0 \tag{10}$$

with I the moment of inertia. The second order time derivative can be discretized by either

$$\ddot{\varphi}^{n+1} = [\varphi^{n+1} - 2\varphi^{n} + \varphi^{n-1}]/\Delta t^2 + O(\Delta t) \tag{11a}$$

or, if a second order accurate fluid solver is used:

$$\ddot{\varphi}^{n+1} = [2\varphi^{n+1} - 5\varphi^{n} + 4\varphi^{n-1} - \varphi^{n-2}]/\Delta t^2 + O(\Delta t^2) \tag{11b}$$

This can be verified by using a Taylor series expansion.

Further experimental verification, the improvement of the accuracy, the increasing of the Reynolds number and the extension to valves with more degrees of freedom and to flexible valves are subjects of current research.

Acknowledgment

We wish to thank D. Palmen for her valuable contributions. This research is supported by the Dutch Technology Foundation (STW), grant nr. EWT58.0857

References

[1] Steenhoven, A.A. van & M.E.H. van Dongen, "Model studies of the closing behaviour of the aortic valve", *J. Fluid Mechanics vol 90*, pp 21—32, 1979

[2] Steenhoven, A.A. van, Van Duppen, Th.J.A.G., Cauwenberg, J.W.G. and Van Renterghem, R.J., "In vitro closing behaviour of Bjork—Shiley, St Jude and Hancock heart valve prostheses in relation to the in vivo recorded aortic valve closure", *J.Biomechanics vol 15*, 1982, pp841—848

[3] Bellhouse, B.J. & L. Talbot, "The fluid mechanics of the aortic valve", *J. Fluid Mechanics vol 35*, pp 721—735

[4] Wippermann, F.K., "On the fluid dynamics of the aortic valve", *J. Fluid Mechanics vol 159*, pp 487—501, 1985

[5] Peskin, C.S., "Numerical analysis of blood flow in the heart", *J. of Comp. Physics vol 25*, pp220—252, 1977

[6] Belytschko, T, "Fluid—structure interaction", *Computers and structures vol 12*, pp459—470,1980

[7] Park, K.C. & C.A. Felippa, "Partitioned analysis of coupled systems", in: T. Belytschko & T.J.R. Hughes (eds.), *Computational methods for transient analysis*, North—Holland, Amsterdam, 1983

[8] Cuvelier, C., A. Segal & A.A. van Steenhoven, *Finite element methods and Navier—Stokes equations*, D. Reidel Publishing Company, Dordrecht, The Netherlands, 1986

[9] Segal, A., *SEPRAN Manual*, Ingenieursbureau SEPRA, Delft, The Netherlands, 1989

[10] Vosse, F.N. van de, A.A. van Steenhoven, A. Segal & J.D. Janssen, " A finite element analysis of the unsteady two—dimensional Navier—Stokes equations", *Int. J. of Numerical Methods in Fluids vol 6*, pp427—443,1986

[11] Vosse, F.N. van de, A.A. van Steenhoven, A. Segal & J.D. Janssen, " A finite element element analysis of the steady laminar entrance flow in a 90^{o} curved tube", *Int. J. of Numerical Methods in Fluids vol 9*, pp275—287,1989

[12] Press, W.H., B.P. Flannery, S.A. Teukolsky & W.T. Vetterling, *Numerical Recipes*, Cambridge University Press, New York, 1986

[13] Brent, R.P., *Algorithms for minimization without derivatives*, Prentice—Hall, Englewood Cliffs, N.J., USA, 1973